Unlimited Sampling for Radar-based Vital Sign Monitoring

Gabriel Beltrão
Interdisciplinary Centre for Security, Reliability and Trust
University of Luxembourg
gabriel.tedgue-beltrao@uni.lu

Thomas Feuillen
Interdisciplinary Centre for Security, Reliability and Trust
University of Luxembourg
thomas.feuillen.research@gmail.com

Bhavani Shankar M.R.
Interdisciplinary Centre for Security, Reliability and Trust
University of Luxembourg
Bhavani.Shankar@uni.lu

Mohammad Alaee-Kerahroodi
Interdisciplinary Centre for Security, Reliability and Trust
University of Luxembourg
mohammad.alaee@uni.lu

Udo Schroeder
Basics and Mathematical Modeling
IEE S.A.
Luxembourg, Luxembourg
udo.schroeder@iee.lu

***Abstract*—This paper tackles the contactless recovery of vital sign information from backscattered signals using a radar device. These sensors do not require any physical contact with the patient, which makes them extremely suitable for healthcare applications such as the long-term monitoring of patients or elderly care. In this context, the information regarding the breathing and heart rate is embedded within the phase of the received radar signal and inherently suffers from a 2π ambiguity. For sensors operating at millimeter-wave, common recovery methods rely on algorithms that unwrap the phase. These methods, however, do not possess strong recovery guarantees and often fail when encountering quick phase variations (e.g., random body movements and larger chest displacements). This can hinder accurate estimation and possibly prevent the proper medical diagnosis. This paper proposes to do away with these limitations by using the framework of Unlimited Sampling (US) to address the recovery of the signal embedded in the phase. Compared to other unwrapping algorithms, the US framework provides perfect recovery guarantees in practical settings. Furthermore, we show through simulations that the US-based recovery algorithm greatly extends the resilience of the recovering process when encountering random body movements at comparable sampling rates.**

***Index Terms*—Breathing, FMCW, heart rate, radar, random body movements, unlimited sampling, vital signs.**

I. Introduction

Due to the rapid aging of the population worldwide, a lot of effort is being dedicated to providing more efficient healthcare solutions. Recently, there has been renewed interest in the contactless monitoring of vital signs such as breathing and heart rate. Continuously monitoring this information is crucial for long-term patient care, especially when conventional cabled or wearable devices cannot be used.

In this context, radar devices are emerging as a promising technology. Radar signals can penetrate through different materials and are not affected by skin pigmentation or ambient light levels. In addition, radar devices preserve privacy [1], and can be low-power and low-cost. These characteristics make radar sensors very suitable for several healthcare applications, including sleep monitoring [2], assisted living [3], diagnosis [4], newborn monitoring [5], and many others.

The information regarding the vital signs is embedded within the phase of the received radar signal and inherently suffers from a 2π ambiguity. For sensors operating at millimeter-wave, recovery methods rely on the arctangent demodulation (AD) [4], [6], [7], which requires an additional unwrap operation to unfold the phase. The conventional unwrap algorithm, however, does not possess recovery guarantees and often fails when encountering quick phase variations, usually caused by interfering random body movements (RBMs) or even larger chest displacements. These recovery errors can hinder accurate estimation and possibly prevent the proper medical diagnosis.

To overcome these limitations, in this paper we propose a new algorithm that uses the framework of Unlimited Sampling (US) [8], [9] to address the recovery of the signal embedded in the phase. Compared to the conventional unwrap algorithm, the US provides perfect recovery guarantees in practical settings [10]–[12]. Furthermore, we show through simulations that the US-based recovery algorithm greatly extends the resilience of the recovering process when encountering random body movements at comparable sampling rates.

The remainder of this paper is organized as follows. In section II, we introduce the signal modeling for vital sign processing using radars. In Section III we describe a widely used unwrap-based phase demodulation method and highlight its limitations. In Section IV we present the US framework and how it can be used to overcome these issues. Finally, in Section V, we show in a simulation setting the gain provided by the US-based recovery algorithm, whereas, in Section VI, a few conclusions are drawn.

This work was supported by the Luxembourg National Research Fund (FNR), under the FNR Industrial Fellowship Grant, project MIDIA, Reference 14269859.

A. Notation

Throughout this paper, we are adopting the following notation: lower case boldface for vectors $\boldsymbol{x}$ and upper case boldface for matrices $\boldsymbol{X}$. The letter j represents the imaginary unit (i.e., $\mathrm{j} = \sqrt{-1}$), with the absolute value given by $|(\cdot)|$. The Euclidean norm of the vector $\boldsymbol{x}$ is denoted by $\|\boldsymbol{x}\|$. For any complex number x we use $\Re$ and $\Im$ to denote, respectively, the real and the imaginary parts of x. The first order difference of a signal $\boldsymbol{s}$ is denoted by $(\Delta \boldsymbol{s})[k] \stackrel{\text{def}}{=} s[k+1] - s[k]$, whereas the N-th order difference $\Delta^N \boldsymbol{s}$ is obtained by the recursive application of the finite-difference operator. Finally, S is the anti-difference operator.

II. Vital Sign Models

The transmitted radar signal is modulated by the subtle chest wall motion due to the breathing and heartbeat mechanisms. The vital sign information is then embedded in the received radar signal as an additional phase modulation related to the chest wall movement. The complex slow-time signal received from the monitored subject at nominal distance d_0 can be represented as

$$s(t) = \exp\left\{\mathrm{j}\left(\theta_0 + \frac{4\pi d(t)}{\lambda}\right)\right\}, \tag{1}$$

where $\theta_0 = 4\pi d_0/\lambda$ is a constant phase shift. The time-varying phase component of the received signal can be written as

$$\frac{4\pi d(t)}{\lambda} = \frac{4\pi}{\lambda}\big(d_{\mathrm{b}}(t) + d_{\mathrm{h}}(t) + d_{\mathrm{rbm}}(t)\big),$$

where λ is the operating wavelength, and $d_{\mathrm{b}}(t)$ and $d_{\mathrm{h}}(t)$ represent the chest wall motion due to the breathing and heartbeat, respectively. The additional body movement is represented by d_{rbm}, with the subscript RBM here to highlight its random and unknown pattern in practical settings. The amplitudes of the chest wall motion vary from 4 to 12 mm when breathing, and 0.2 mm to 0.5 mm when the heart beats [13]. At rest, the standard physiological range of the breathing rate goes from 10 to 25 breaths per minute, whereas, for the heart rate, it goes from 60 to 100 beats per minute.

In ideal conditions, perfect recovery of the chest wall motion $d(t)$ would allow for precise estimation of the breathing and heart rates by simple analysis of the movement periodicity. However, in practice, the received radar signal is usually tainted by reflections from the external environment and additional RBMs from the monitored subject. These interfering signals are usually much stronger than those induced by the chest wall millimeter displacement, thus rendering the accurate recovery of vital signs challenging. It is important to note these RBMs cannot be avoided in practical situations. Therefore, contactless monitoring can only reach its full potential if it can be seamlessly integrated without added restrictions on the patients. This is why developing methods that are robust to large RBMs is of paramount importance for radar-based monitoring of vital signs [14]–[16].

III. Phase Demodulation

Phase demodulation is essentially the process where the complex samples of the slow-time signal are combined, in order to recover the displacement signal from the phase variation over time. Several techniques have already been proposed for that, including the complex-signal demodulation (CSD) [17]–[19] and the linear demodulation [20]–[22]. As discussed in [23], these methods suffer from intermodulation products and harmonic interference when working at higher operating frequencies. To avoid these issues and enable precise phase recovery, the AD is commonly used. In this case, the recovered displacement signal can be obtained using

$$\widehat{d}(t) = \frac{\lambda}{4\pi} \cdot \mathrm{unwrap}\left(\arctan\left[\frac{\Im(s(t))}{\Re(s(t))}\right]\right).$$

As the phase is bounded by $[-\pi, \pi]$, displacements larger than $\lambda/4$ will result in discontinuities. To reconstruct the phase and estimate the signal of interest, the AD requires an additional unwrap operation.

The conventional unwrap algorithm is commonly used, and it has a very straightforward implementation. Whenever the phase jump between two consecutive samples is greater than or equal to π radians, it corrects the new sample by adding $\pm 2\pi$, so that the difference becomes less than π. However, this algorithm is very sensitive to interference. It often fails when dealing with signals that exhibit quick phase variations, which can be due to RBMs or even faster chest displacements. In these cases, unwrap errors can be accumulated and result in large distortions in the recovered displacement signal. Figure 1 shows a 20-second segment of a simulated chest wall displacement signal, contaminated with a short segment of RBM interference. Initially, when only the breathing and heartbeat signals are present, the wrapped phases can be accurately recovered. However, in the presence of additional RBMs, the conventional unwrap fails and large distortions are then introduced in the recovered signal.

The well-known Itoh's condition [24] defines theoretical bounds for the performance of the conventional unwrap algorithm. It states that a necessary condition for successfully recovery is that the maximum amplitude of the first-order difference of input samples should be limited by λ. In other words, the maximum phase (displacement) variation between adjacent time samples should be smaller than the operating wavelength, *i.e.*

$$\forall k \in [K], \big|d[k+1] - d[k]\big| \leqslant \lambda, \tag{2}$$

where k is the sample index for a signal with K samples. If this is satisfied, phase changes greater than π indicate that the phase should be corrected simply by adding or subtracting 2π. Increasing the sampling frequency will generate highly correlated samples with a lower first-order difference. So the performance of conventional unwrap is dependent on the slow-time sampling frequency. This can usually lead to substantial oversampling. However, Itoh's condition is a necessary but not sufficient condition for successful reconstruction. Under

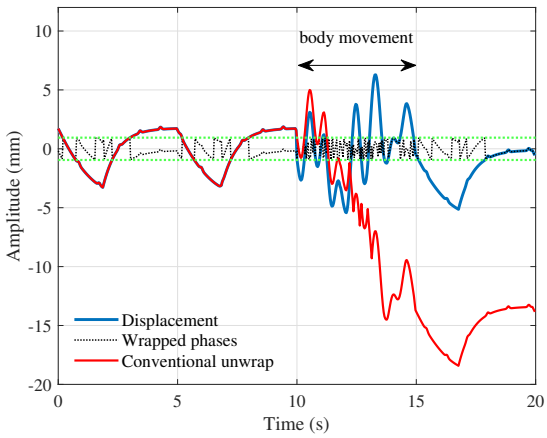

Figure 1: Chest wall displacement contaminated with additional body movement: true displacement, wrapped phases around $\pm\lambda/2$, and recovered signal using the conventional unwrap algorithm.

practical settings and reasonable amplitude of random body movements, the conventional unwrap operation used in the AD completely fails to recover the chest wall displacement signal.

IV. Unlimited Sampling

The previous section introduced the inherent challenge that arises when estimating vital signs from radar measurements, *i.e.*, the information of interest is embedded in the phase of the received signal. Considering the limitations of the classic unwrap method, we introduce here the use of the US framework for recovering the vital sign information.

The US is a novel framework that breaks away from the limitations of the classic unwrapping method, that is Itoh's condition, by leveraging the fact that the signals of interest are bandlimited. It was originally proposed for tackling analog-to-digital converter (ADC) saturation by co-designing the sensing architecture and the algorithms that fold the signal; thus giving an *unlimited* dynamic range. Earlier publications [10]–[12] first demonstrated theoretical recovery capabilities using US-enabled devices, whereas recent publications are demonstrating its potential in real settings [25]–[27]. In this work, we leverage this new framework in the context of recovering the phase for radar-based monitoring of vital signs.

Let us consider the following acquisition model. Let $g(t) := 2d(t)$ be the signal of interest, sampled at a rate $\frac{1}{T}$, using a modulo-based acquisition system $\mathscr{M}_\lambda(\cdot)$ with a dynamic range of λ ($\pm\lambda/2$). The acquired folded signal is thus

$$y[k] = \mathscr{M}_\lambda(g(kT)), \tag{3}$$

where the link between (3) and (1) is given by

$$\mathscr{M}_\lambda(g(kT)) = \frac{\lambda}{2\pi}\angle s(kT),$$

with $\frac{1}{T}$ being the slow-time sampling rate. While the conventional unwrap only has a necessary condition for reconstruction, the US provides the following result:

Theorem 1 (Unlimited Sampling Theorem, [12])**.** *Let $g(t)$ be a finite energy, bandlimited signal with maximum frequency Ω and let $y[n]$, $n \in \mathbb{Z}$ in (3) be the modulo samples of $g(t)$ with sampling rate $\frac{1}{T}$. Then a sufficient condition for the recovery of $g(t)$ from $y[n]$ is that $T \leqslant \frac{1}{2\Omega e}$ (up to additive multiples of 2λ) where e denotes Euler's constant.*

It is interesting to see that the sampling rate $\frac{1}{T}$ required for perfect reconstruction neither depends on the amplitude of the signal nor, and more strikingly, on the dynamic range λ used for the folded acquisition (*e.g.* the radar's wavelength). Herein lies the main advantage of using the US framework; only the knowledge that the signal is bandlimited is sufficient to guarantee its perfect reconstruction. One can also see the result in Theorem 1 as an extension of the Nyquist sampling theorem to folded signals. Along with this result, the authors in [12] also developed an iterative reconstruction algorithm that provides perfect estimates $\widetilde{d}[k]$ from the folded measurements $y[k]$.

Algorithm 1: Unlimited Sampling Algorithm

Data: $y[k]$ and $\lambda\mathbb{Z} \ni \beta_r \geqslant 2\|d\|_\infty$.
Result: $\widetilde{d}[k] \approx d[k]$.
1) Compute $N = \left\lceil \frac{\log\lambda/2 - \log\beta_r}{\log(T\Omega e)} \right\rceil$.
2) Set $z_{(0)}[k] = \left(\mathscr{M}_\lambda(\Delta^N y) - \Delta^N y\right)[k]$.
3) for $n = 0 : N-2$
   (i) $z_{(n+1)}[k] = \left(\mathsf{S}z_{(n)}\right)[k]$.
   (ii) $z_{(n+1)} = \lambda \left\lceil \frac{\lfloor 2z_{(n+1)}/\lambda \rfloor}{2} \right\rceil$ (rounding to $\lambda\mathbb{Z}$).
   (iii) With $J = 12\beta_r/\lambda$, compute κ_n.
   $\kappa_n = \left\lfloor \frac{\mathsf{S}z_{(n+1)}[1] - \mathsf{S}z_{(n+1)}[J+1]}{24\beta_r} + \frac{1}{2} \right\rfloor$
   (iv) $z_{(n+1)}[k] = z_{(n+1)}[k] + \lambda\kappa_{(n)}$.
   end
4) $\widetilde{d}[k] = \frac{1}{2}\left[\left(\mathsf{S}z_{(N-1)}\right)[k] + y[k] + m\lambda\right], \quad m\mathbb{Z}$.

This algorithm relies on the fact that finite differences and modulo operations can somewhat commute at high order [12, Prop. 2]. In this sense, one can also see the US framework as an extension of Itoh's condition to higher orders.

Finally, the recovered displacement signal using the US-based recovery can be expressed as

$$\widehat{d}(t) = \mathrm{US}\left(\frac{\lambda}{2\pi}\arctan\left[\frac{\Im(s(t))}{\Re(s(t))}\right]\right),$$

where the US operator represents a function that executes the US algorithm.

V. Simulation Results

In order to assess the performance gain provided by the proposed US-based recovery method, Monte Carlo simulations were carried out.

Based on [28], the chest wall displacement due to breathing $d_\mathrm{b}(t)$ is modeled as a low-pass filtered periodic sequence of quadratic inspiration and exponential expiration. For modeling the heartbeat displacement $d_\mathrm{h}(t)$, a Gaussian pulse train is

used [29], based on the idea that the heartbeat is a short explosive motion with a pulsatile nature. The initial phase of both displacements is generated randomly on each run. As an example, the breathing rate and amplitude were defined as 13 bpm and 12 mm, respectively, whereas for the heartbeat, we used 70 bpm and 0.5 mm, respectively.

The RBM interfering signal $d_{\text{rbm}}(t)$ is constructed using three different models related to different types of body movements:

- First, the *ramp* body movement was defined as

$$d_{\text{rbm}}(t) = a_{\text{rbm}} \frac{(t - t_i)}{(t_f - t_i)},$$

  where a_{rbm} is the movement's amplitude, and $t \in [t_i, t_f]$, with t_i and t_f being the initial and final time of the movement, respectively. This model could represent, for instance, a simple torso movement to the front.
- The second body movement follows a *sine* function and is defined as

$$d_{\text{rbm}}(t) = a_{\text{rbm}} \sin\left(2\pi f_{\text{rbm}}(t - t_i) + \phi\right),$$

  where f_{rbm} is the movement's frequency and $\phi \in \mathcal{U}(-\pi, \pi)$ is the random initial phase. Here we are modeling a rocking (back-and-forth) motion of the torso, with controllable amplitude and frequency.
- And finally, the *fully random* body movement, which is defined as

$$d_{\text{rbm}}(t) = a_{\text{rbm}} \frac{z(t)}{\|z(t)\|_\infty},$$

  where $z(t)$ is a real signal whose spectrum is bandlimited at f_{rbm}, with each component of the non-zero spectrum being of unit amplitude with a random phase in $[0, 2\pi]$. This model does not impose any particular structure and more closely resembles an actual interfering body motion.

Figure 2 shows examples of the displacements generated by these models. The purpose of using these different models is twofold. First, by using the first and second models, we show that our approach can deal with body movements that are commonly occurring in day-to-day life and that can be easily modeled. Second, to avoid narrowing our study to specific movements, and to properly showcase the resilience of the US recovery to a broad range of movements, the *fully random* movement is used. Indeed, actual body movements have an inherent limit in their frequency content as they do not exhibit infinite acceleration. This makes the bandlimited RBM model appealing as it fits both the physics of the problem and the requirement of Theorem 1.

The composite displacement signal $d(t)$ is low-pass filtered and used to generate the slow-time complex samples according to (1), with the phase shift θ_0 being modeled as a random variable, *i.e.* $\theta_0 \in \mathcal{U}(-\pi, \pi)$. At each iteration, the generated signal is processed using the AD with the conventional unwrap operation or the proposed US-based recovery. From now on, we will refer to these methods simply as AD or US, respectively.

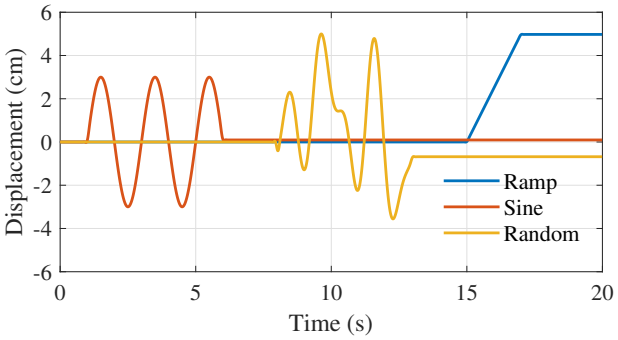

Figure 2: Illustration of simulated body movements.

The reconstruction is tested for different amplitudes of the RBM, as well as for different slow-time sampling rates, in a Monte Carlo approach. The normalized recovery error (NRE) is then calculated as

$$\text{NRE} = 10 \log_{10}\left(\frac{\|\boldsymbol{d} - \widehat{\boldsymbol{d}}\|}{\|\boldsymbol{d}\|}\right),$$

where $\boldsymbol{d}$ and $\widehat{\boldsymbol{d}}$ represent the vectors with the true and recovered displacement signals, respectively. The final performance for each method is evaluated by averaging the NRE over all iterations, with 1000 runs being performed for each scenario. In this initial work, we are only evaluating the noiseless case.

Figure 3 shows the average NRE as a function of the slow-time sampling frequency and RBM amplitude, considering all the three simulated body movements, using an operating frequency of $f_c = 60$ GHz ($\lambda = 5$ mm). For easy interpretation of the results, the blue areas represent a perfect recovery of the displacement signal, while the red ones indicate regions of failure. The duration of the processing window was 20 seconds, and each movement started at the tenth second, with a duration of 2 seconds.

Figure 3a shows the performance of conventional unwrap for the *ramp* body movement. It can be seen that it follows the linear behavior stated in (2), *i.e.*, for precise phase recovery, the slow-time sampling rate needs to be increased linearly according to the amplitude of the interfering body movement. Figure 3d shows the performance when using the US framework. In this case, for recovering RBMs with the same amplitude, a much smaller slow-time sampling frequency can be used. In fact, after reaching a minimum value for the slow-time sampling frequency, the proposed algorithm can precisely recover the displacement signal, independent of the RBM amplitude. The required sampling for perfect reconstruction only depends on the bandwidth of the signal of interest (not on its amplitude), which is consistent with Theorem 1.

Figures 3b and 3c show the performance of conventional unwrap for the *sine* and *fully random* body movements, with $f_{\text{rbm}} = 0.3$ Hz. In these cases, given the more complex behavior of the additional interference, even smaller amplitudes of RBMs completely prevent successful recovery of the displacement signal, which would require much higher sampling rates. On the other hand, it can be seen in Figs. 3e and

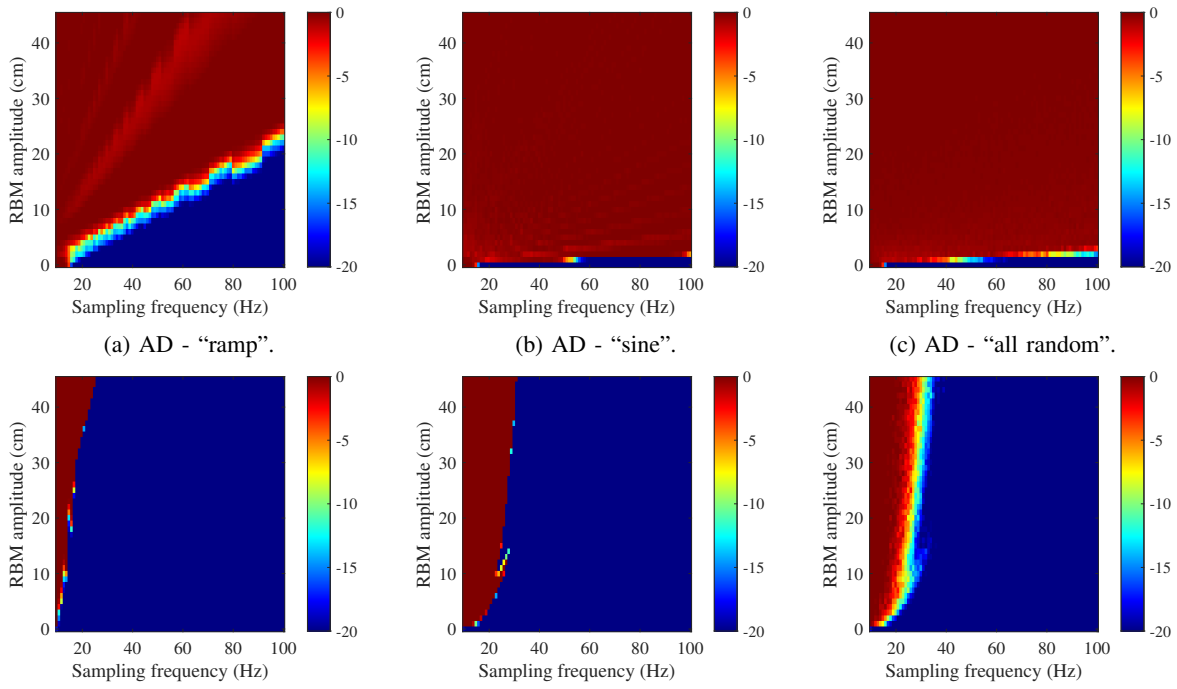

(a) AD - "ramp". (b) AD - "sine". (c) AD - "all random".

(d) US - "ramp". (e) US - "sine". (f) US - "all random".

Figure 3: Normalized recovery error (in dB) for different body movements.

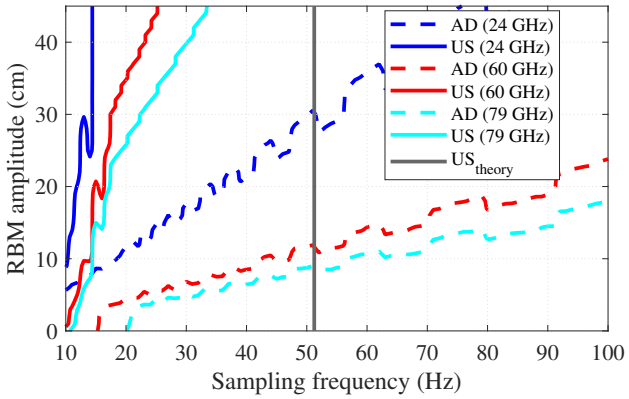

Figure 4: Normalized recovery error (threshold at -20 dB) for the ramp body movement, at different operating frequencies.

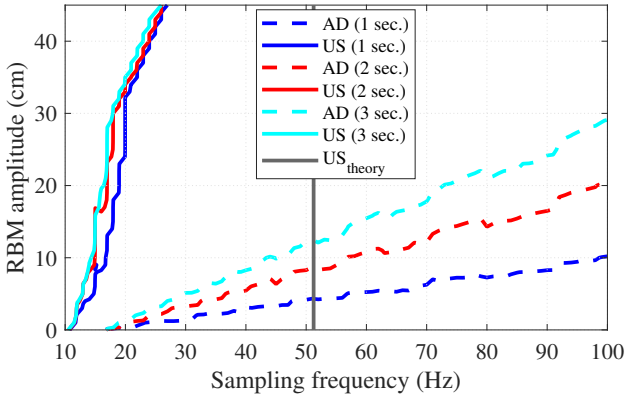

Figure 5: Normalized recovery error (threshold at -20 dB) for the ramp body movement, with different durations.

3f, that the US-based method provides a large improvement compared to conventional unwrap, with minor degradation at larger amplitudes of the RBM. It only fails when the slow-time sampling frequency is lower than 20 Hz and 30 Hz for the *sine* and *fully random* body movements, respectively. Therefore, it extends the resilience of the recovery process when encountering random body movements at comparable sampling rates.

It is important to mention that, if f_{rbm} does not overlap with vital sign frequencies, accurate recovery of the displacement signal using the US would allow easy filtering of the RBM interference by conventional spectral analysis. However, incorrect demodulation using the conventional unwrap algorithm may introduce nonlinear errors that can hinder filtering and prevent subsequent estimation, even under the simplest RBM interference.

Figure 4 shows -20 dB threshold lines in the NRE (perfect recovery below the lines), for the *ramp* body movement with the same parameters as before, now at different operating frequencies. It can be seen that, under the RBM interference, the AD performance decreases at higher operating frequencies. At 60 GHz and 79 GHz for instance, the AD cannot recover RBMs with amplitudes larger than 20 cm, even if oversampling at 100 Hz. Conversely, the US method provides

perfect recovery of a 20 cm RBM using a slow-time sampling frequency lower than 25 Hz or 35 Hz, at 60 GHz and 79 GHz, respectively.

Finally, Fig. 5 shows the -20 dB threshold lines for the same *ramp* body movement, but now with different durations. Reducing the duration to reach the same amplitude is equivalent to increasing the movement velocity. In these cases, the AD with conventional unwrap follows Itoh's condition with performance degradation at higher velocities, whereas unwrapping with the US method is independent of the velocity variation and can provide perfect recovery until 45 cm with less than 30 Hz of slow-time sampling frequency. This sampling rate is also below the upper-bounded sampling rate predicted by Theorem 1 represented by the gray line in Fig. 4 and Fig. 5.

VI. Conclusion

We proposed in this paper the use of a novel framework for recovering vital signs from radar measurements. The proposed method relies on the US framework, for being able to tackle the recovery of signals whose measurements are folded. We first introduced the AD with the conventional unwrap operation, which has limitations to recover the embedded phase, especially under the presence of interfering body movements. Leveraging the fact that these movements are, because of their human nature, bandlimited, we showed that the US provides an attractive alternative for the successful recovery of the displacement signal. The simulation results confirmed that the required sampling rate for the US to succeed was far inferior to the conventional unwrap and, more importantly, independent of the amplitude of the movement. Future work will extend this initial analysis to noisy scenarios and, further, to practical measurements using radar sensors.

References

[1] Y. Zhang, F. Qi, H. Lv, F. Liang, and J. Wang, "Bioradar Technology: Recent Research and Advancements," *IEEE Microw. Mag.*, vol. 20, no. 8, pp. 58–73, aug 2019.

[2] M. Zakrzewski, A. Vehkaoja, A. S. Joutsen, K. T. Palovuori, and J. J. Vanhala, "Noncontact Respiration Monitoring During Sleep With Microwave Doppler Radar," *IEEE Sens. J.*, vol. 15, no. 10, pp. 5683–5693, oct 2015.

[3] D. F. Fioranelli, D. S. A. Shah, H. Li1, A. Shrestha, D. S. Yang, and D. J. L. Kernec, "Radar sensing for healthcare," *Electron. Lett.*, vol. 55, no. 19, pp. 1022–1024, sep 2019.

[4] Wei Hu, Zhangyan Zhao, Yunfeng Wang, Haiying Zhang, and Fujiang Lin, "Noncontact Accurate Measurement of Cardiopulmonary Activity Using a Compact Quadrature Doppler Radar Sensor," *IEEE Trans. Biomed. Eng.*, vol. 61, no. 3, pp. 725–735, mar 2014.

[5] G. Beltrão *et al.*, "Contactless radar-based breathing monitoring of premature infants in the neonatal intensive care unit," *Sci. Rep.*, vol. 12, no. 1, pp. 1–15, 2022.

[6] B.-K. Park, O. Boric-Lubecke, and V. M. Lubecke, "Arctangent Demodulation With DC Offset Compensation in Quadrature Doppler Radar Receiver Systems," *IEEE Trans. Microw. Theory Tech.*, vol. 55, no. 5, pp. 1073–1079, may 2007.

[7] T. Sakamoto, R. Imasaka, H. Taki, T. Sato, M. Yoshioka, K. Inoue, T. Fukuda, and H. Sakai, "Feature-based Correlation and Topological Similarity for Interbeat Interval Estimation using Ultra-Wideband Radar," *IEEE Trans. Biomed. Eng.*, vol. 63, no. 4, pp. 1–1, 2015.

[8] A. Bhandari, F. Krahmer, and R. Raskar, "On unlimited sampling," *2017 12th Int. Conf. Sampl. Theory Appl. SampTA 2017*, pp. 31–35, 2017.

[9] ——, "On Unlimited Sampling and Reconstruction," *IEEE Trans. Signal Process.*, vol. 69, pp. 3827–3839, 2021.

[10] ——, "On unlimited sampling," in *2017 International Conference on Sampling Theory and Applications (SampTA)*, 2017, pp. 31–35.

[11] ——, "Unlimited sampling of sparse signals," in *2018 IEEE International Conference on Acoustics, Speech and Signal Processing (ICASSP)*, 2018, pp. 4569–4573.

[12] ——, "On unlimited sampling and reconstruction," *IEEE Transactions on Signal Processing*, vol. 69, pp. 3827–3839, 2021.

[13] M. Kebe, R. Gadhafi, B. Mohammad, M. Sanduleanu, H. Saleh, and M. Al-qutayri, "Human vital signs detection methods and potential using radars: A review," *Sensors (Switzerland)*, vol. 20, no. 5, 2020.

[14] Q. Lv, L. Chen, K. An, J. Wang, H. Li, D. Ye, J. Huangfu, C. Li, and L. Ran, "Doppler Vital Signs Detection in the Presence of Large-Scale Random Body Movements," *IEEE Trans. Microw. Theory Tech.*, vol. 66, no. 9, pp. 4261–4270, sep 2018.

[15] S. A. Shah and F. Fioranelli, "RF Sensing Technologies for Assisted Daily Living in Healthcare: A Comprehensive Review," *IEEE Aerosp. Electron. Syst. Mag.*, vol. 34, no. 11, pp. 26–44, 2019.

[16] G. Beltrão, M. Alaee-Kerahroodi, U. Schroeder, and M. R. B. Shankar, "Joint Waveform/Receiver Design for Vital-Sign Detection in Signal-Dependent Interference," in *IEEE Radar Conf.*, 2020, pp. 1–6.

[17] Changzhi Li and Jenshan Lin, "Random Body Movement Cancellation in Doppler Radar Vital Sign Detection," *IEEE Trans. Microw. Theory Tech.*, vol. 56, no. 12, pp. 3143–3152, dec 2008.

[18] K. Naishadham, J. E. Piou, L. Ren, and A. E. Fathy, "Estimation of Cardiopulmonary Parameters From Ultra Wideband Radar Measurements Using the State Space Method," *IEEE Trans. Biomed. Circuits Syst.*, vol. 10, no. 6, pp. 1037–1046, dec 2016.

[19] R. Qian, T. Jin, H. Li, and Y. Dai, "WT-Based Data-Length-Variation Technique for Fast Heart Rate Detection," in *2018 Prog. Electromagn. Res. Symp.*, vol. 66, no. 1. IEEE, aug 2018, pp. 399–404.

[20] W. Massagram, V. M. Lubecke, A. Høst-Madsen, and O. Boric-Lubecke, "Assessment of heart rate variability and respiratory sinus arrhythmia via doppler radar," *IEEE Trans. Microw. Theory Tech.*, vol. 57, no. 10, pp. 2542–2549, 2009.

[21] M. Mercuri, I. R. Lorato, Y.-H. Liu, F. Wieringa, C. V. Hoof, and T. Torfs, "Vital-sign monitoring and spatial tracking of multiple people using a contactless radar-based sensor," *Nat. Electron.*, vol. 2, no. 6, pp. 252–262, jun 2019.

[22] M. Mercuri, Y. Lu, S. Polito, F. Wieringa, Y.-H. Liu, A.-J. van der Veen, C. Van Hoof, and T. Torfs, "Enabling Robust Radar-Based Localization and Vital Signs Monitoring in Multipath Propagation Environments," *IEEE Trans. Biomed. Eng.*, vol. 68, no. 11, pp. 3228–3240, nov 2021.

[23] G. Beltrão, M. Alaee-Kerahroodi, U. Schroeder, D. Tatarinov, and M. R. Bhavani Shankar, "Statistical performance analysis of radar-based vital-sign processing techniques," *Sensing Technology*, pp. 101–112, 2022.

[24] K. Itoh, "Analysis of the phase unwrapping algorithm," *Applied optics*, vol. 21, no. 14, pp. 2470–2470, 1982.

[25] A. Bhandari, F. Krahmer, and T. Poskitt, "Unlimited sampling from theory to practice: Fourier-prony recovery and prototype adc," *IEEE Transactions on Signal Processing*, vol. 70, pp. 1131–1141, 2022.

[26] D. Florescu, F. Krahmer, and A. Bhandari, "The surprising benefits of hysteresis in unlimited sampling: Theory, algorithms and experiments," *IEEE Transactions on Signal Processing*, vol. 70, pp. 616–630, 2022.

[27] T. Feuillen, M. Alaee-Kerahroodi, A. Bhandari, B. S. M. R, and B. Ottersten, "Unlimited sampling for fmcw radars: A proof of concept," in *2022 IEEE Radar Conference (RadarConf22)*, 2022, pp. 1–5.

[28] A. Albanese, L. Cheng, M. Ursino, and N. W. Chbat, "An integrated mathematical model of the human cardiopulmonary system: model development," *Am. J. Physiol. Circ. Physiol.*, vol. 310, no. 7, pp. H899–H921, apr 2016.

[29] M. Nosrati and N. Tavassolian, "High-Accuracy Heart Rate Variability Monitoring Using Doppler Radar Based on Gaussian Pulse Train Modeling and FTPR Algorithm," *IEEE Trans. Microw. Theory Tech.*, vol. 66, no. 1, pp. 556–567, jan 2018.